

THE BALLISTIC PARTICLE MODEL AND THE VERTEX DEVIATION OF YOUNG STARS NEAR THE SUN

JAMES L. HILTON AND FRANK BASH

Department of Astronomy, University of Texas at Austin

Received 1981 April 13; accepted 1981 October 15

ABSTRACT

We have examined the connection between the initial motions, at birth, of O and B stars and the long-standing problem of the vertex deviation. The ballistic particle model for spiral arm star formation is used to predict the velocities of young stars near the Sun. The model is seen to be consistent with observations in that it predicts that O and B stars will have a distribution of velocities in which the direction of maximum velocity dispersion points toward $l \approx 320^\circ$. The predicted values of the vertex deviation away from the galactic center and the velocity centroid with respect to the dynamical, local standard of rest are very near the observed values.

The sense of the vertex deviation, predicted by the model, is seen to be caused by the assumption that the stars form from dense molecular clouds launched from the spiral arms at the postshock velocity which has a radial component directed toward the galactic center. With the radial component of the initial velocities directed away from the center, the vertex deviates toward the direction of increasing galactic longitude.

Complications due to the effect of the second harmonic resonance in the gas and star formation along the Orion spur are discussed. The model includes neither of these as sources of young stars within 2 kpc of the Sun.

Subject headings: galaxies: Milky Way — stars: early-type — stars: stellar dynamics

I. INTRODUCTION

The ballistic particle model devised by Bash and Peters (1976) and refined by Bash, Green, and Peters (1977) and Bash (1979) predicts the initial velocities of stars which have been born in the spiral arm. The model has been compared with several different observations in previous papers. Here, we examine its predictions of the velocities of young stars near the Sun.

The distribution of velocities of stars near the Sun has been studied for nearly a century. In general, stars are seen to have a maximum velocity dispersion along a line lying in the galactic plane and pointing roughly toward the galactic center. Early-type stars, however, are unusual in that the direction of largest velocity dispersion points a long way from the galactic center. That is, they show a large “vertex deviation.”

Kapteyn (1900, 1922) suggested that stellar motions near the Sun could be represented by two star streams, in each of which the random motions could be represented by a spherical distribution. Schwarzschild (1908) suggested a simpler and more elegant description—that the random motions of stars near the Sun could be described by a velocity ellipsoid. Two of the principal axes of this ellipsoid are found to lie in the galactic plane, and these two axes are the only ones which concern us here since our model describes stellar orbits only in the plane. For main-sequence stars, the deviation of the velocity ellipse is almost constant for early B stars ($l \approx 320^\circ$) and then rapidly increases to $l \approx +25^\circ$ for A0 stars; the deviation of the velocity ellipse then decreases slowly for later

spectral type, and hence greater average age stars (ellipse points at $l \approx 5^\circ$ at M). The explanations for the deviation of the major axis of the velocity ellipse fall into two major categories: the steady state theories and the initial condition theories.

In the steady state theories, a perturbation in the “flow” of stars around the galactic center is pictured. This perturbation is often associated with the spiral structure, and it may offer an explanation for the vertex deviations of later type stars, but these theories do not explain why O and B stars should behave so differently from later type stars. The first steady state theories were discussed by Oort (1928) and Lindblad (1927), who contended that the deviation required a third integral of motion in addition to energy and angular momentum. Mayor (1970) attributed the deviation of the velocity ellipse to age-independent perturbation of the residual velocities by the spiral structure. However, he concerned himself with only late-type stars for which the deviation is nearly constant with spectral type. In contrast, Heckmann and Strassl (1934) proposed that the deviation of the velocity ellipse was caused by random local irregularities in the velocity distribution of the stars; however, the change in the orientation of the velocity ellipse with spectral type and therefore average stellar age does not appear to be random but a smooth function of age. House and Innanen (1975) showed the possibility that the change in the ellipse with stellar age could be caused by the random motions of stars; however, they predict no significant vertex deviation for the first 10^8 years, and the

youngest stars do show the greatest deviation (see Nordström 1936).

The initial condition theories such as that given by Yuan (1971), on the other hand, argue that the deviation of the velocity ellipse is caused by the initial velocities the stars had at their birth. In order to show this, he integrated the trajectory of stars, backward in time, using a gravitational potential model developed by Yuan (1969), to show how the ellipse will change with age.

Woolley (1970) showed observationally that the change of the deviation of the velocity ellipse is a function of the average age of stars in the sample and is not a phenomenon caused by random local perturbations of stellar velocities, but he did not predict what initial conditions caused the observed ellipse.

The initial condition theories have the advantage of predicting that early-type stars should show different kinematics from that of late-type ones, but the initial velocities were unknown.

None of the steady state models have been able to explain the observed deviation of the velocity ellipse, nor have the initial condition papers tried to start with a set of initial conditions and predict the velocity ellipse from them.

II. THE GALACTIC MODEL

The ballistic particle model suggests that spiral arm stars are born in dense molecular clouds and that the clouds are launched from the two-armed spiral shock wave at the postshock velocity. The model assumes that the clouds, and the stars born in the clouds, have galactic orbits which can be integrated where the only influence on those orbits is the gravity of the whole Galaxy, perturbed by the mass concentrated in the density wave arms. These clouds and their stars are hereafter called "ballistic particles" or "particles." In this model, the particles are launched off the spiral arms with postshock initial velocities determined by a hydrodynamic code and are given an initial dispersion of $\pm 5 \text{ km s}^{-1}$ in both the radial and tangential directions. A separate model was generated with particles launched from the arms with preshock initial velocities, which the hydrodynamic code also generates, to see if preshock velocities might give a better fit to observations as in the case of the work on M51 by Wielen (1977). The initial velocities in this case were also given a velocity dispersion of $\pm 5 \text{ km s}^{-1}$ in both directions. The tangential components of the initial velocities from the hydrodynamic program are seen to be about 20 km s^{-1} slower than the circular velocity, in both the preshock and postshock cases. Thus, these cases differ only in the radial component of the initial velocity. Preshock initial velocities have a radial component of about 15 km s^{-1} away from the galactic center, while postshock ones are about 10 km s^{-1} toward the center. The model includes as free parameters the age of a molecular cloud at which the stars which formed in it reach the zero-age main sequence, the solar position in the Galaxy, with respect to the nearby spiral arms, and the expected main-sequence lifetime for the stars. We also need an estimate of the main-sequence lifetimes for stars

TABLE 1
STELLAR MAIN SEQUENCE FOR EARLY B STARS

Spectral Type	Age (10^6 yr)
O9	6
B0	9
B1	11
B2	15
B3	22
B4	57
B5	64

of various spectral types; these lifetimes are varied up and down.

The integration of the particle orbits furnishes the particle's position and velocity as a function of the time since its birth in the spiral arms. The position of the density wave arms is that given in Bash, Green, and Peters (1977). The particles were broken into five age categories: $0-9 \times 10^6$ yr, $10-15 \times 10^6$ yr, $16-22 \times 10^6$ yr, $23-57 \times 10^6$ yr, and $58-64 \times 10^6$ yr, starting from age zero at stellar birth, according to the expected main-sequence lifetimes of spectral types B0-B5 stars obtained from main-sequence lifetime versus mass calculations of Cester (1965) and Strothers (1974). The adopted main-sequence lifetimes are listed in Table 1. The particles in the galactic model are evenly distributed with respect to age, but the stars in the solar vicinity are not, so each age range was weighted according to the percentage of stars which are seen to lie in that age range from the observed sample with whose vertex deviation we are comparing our model (Filin 1957). Figure 1 shows the distribution with respect to spectral type of the Filin sample. We weight the particles in the model on the assumption that

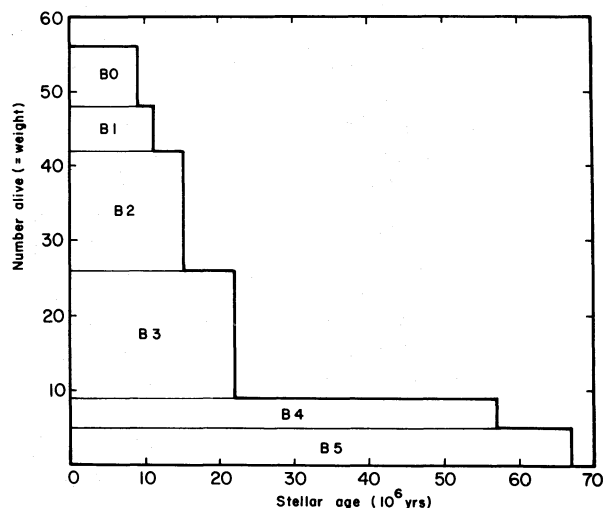


FIG. 1.—The weighting scheme for the model particles as a function of their age. The ordinate is the number of stars left alive at the age shown on the abscissa. The boxes labeled with a spectral type have a width equal to the adopted lifetime and an area equal to the number of stars of that type in the Filin (1957) sample. The weight is the number left alive, assuming each spectral type is born simultaneously, and the weight is represented by the heavy line.

all the stars in the Filin sample were born at the same time after leaving the spiral arms. The weighting assumes that, while stars of the earliest spectral types are alive, so are all the stars of later spectral types. Later, the earliest type stars will die, and, for a given ensemble of stars which were born together, there will be fewer stars.

The motions of the ballistic particles with respect to the dynamical local standard of rest were then computed. The dispersion of the weighted velocities of the ballistic particles was then calculated for the two velocity components in the galactic plane using a method found in Woolley (1970). First, an average of the velocities in the $\tilde{\omega}$ direction, the radial direction away from the galactic center, and in the θ direction, the direction of galactic rotation, are found. Then, the motion of the dynamical local standard of rest is subtracted from the average motion. The resulting velocities are π and θ_1 respectively. The variances are

$$\sigma_{\pi}^2 = \frac{\hat{\Sigma} R_n (\pi - \bar{\pi})^2}{\hat{\Sigma} R_n}, \quad \sigma_{\theta_1}^2 = \frac{\hat{\Sigma} R_n (\theta_1 - \bar{\theta}_1)^2}{\hat{\Sigma} R_n},$$

and

$$\sigma_{\pi\theta_1}^2 = \frac{\hat{\Sigma} R_n (\pi - \bar{\pi})(\theta_1 - \bar{\theta}_1)}{\hat{\Sigma} R_n},$$

where R_n is the weighting factor for each ballistic particle described above. From these three quantities, the lengths of the axes, a and b , of the velocity ellipse and the deviation of the long axis with respect to the direction of the center of the Galaxy, ϕ , may be calculated:

$$a = \sigma_{\theta_1}^2 \cos^2 \phi + 2\sigma_{\pi\theta_1}^2 \cos \phi \sin \phi + \sigma_{\pi}^2 \sin^2 \phi,$$

$$b = \sigma_{\theta_1}^2 \sin^2 \phi - 2\sigma_{\pi\theta_1}^2 \cos \phi \sin \phi + \sigma_{\pi}^2 \cos^2 \phi,$$

$$\phi = \frac{1}{2} \arctan \frac{2\sigma_{\pi\theta_1}^2}{\sigma_{\theta_1}^2 - \sigma_{\pi}^2}.$$

These are the quantities which are compared to observations since observed velocity distributions are not available.

The computer program was checked by inputting artificial data generated with known parameters and finding that those parameters were recovered by the program.

Following the discussion of the results in § IV, a Keplerian approximation is discussed in order to give a qualitative physical feel for the model and its results.

III. RESULTS

In the ballistic particle model, the Sun is located at $R = 10$ kpc from the galactic center. The Perseus arm, outside the Sun, crosses the line connecting the Sun and the galactic center at $R = 11.7$ kpc, and the Sagittarius arm crosses that line inside the Sun at $R = 8.11$ kpc.

The galactic model does not include any contributions from a second spiral shock that is predicted to occur at galactic radii greater than 10.7 kpc. This second shock is caused by a secondary harmonic resonance in the interstellar gas (Shu, Milione, and Roberts 1973) and passes

well inside the 2 kpc radius used to define the solar neighborhood. The exact strength of this secondary shock wave and whether or not dense clouds are ejected from it are not known. Fortunately, the uncertainties involved with the secondary shock wave do not affect the results for the velocity ellipse for this model because the initial velocities of the molecular clouds launched off this secondary arm would carry them outside the solar neighborhood before star formation can occur, given any reasonable time delay from cloud formation to star formation in the cloud.

The Sun is located near a spur, the Orion spur, probably coming off the inner, Sagittarius, arm of the Galaxy and passing within a few hundred parsecs of the Sun in the negative θ direction. This spur contains a fairly large number of stars of spectral type B2 and later. The spur, which is not included in our model of the Galaxy, contributes many of the stars used in observational samples, and, therefore, the resulting velocity ellipse is strongly affected by the motions of the stars from it. However, the spur seems to have been inactive in star formation for the last several million years, and so there are very few (~ 40) main-sequence stars of spectral type B1 or earlier in the Orion spur (Lesh 1968, 1972). Filin (1957) did a study of the velocity dispersion for main-sequence stars of spectral types B0 through B5 and noticed a lack of nearby spectral type B0 and B1 stars as well, but he found 180 spectral type B0 and B1 stars in the main spiral arms of the Galaxy. We then divided the stars into three groups according to spectral type and computed a velocity ellipse for each group. The results of his study are given in Table 2.

Figure 2, which shows B0 and B1 stars, gives the positions in velocity space of the particles with ages from 36 to 47 million years, which corresponds to stellar ages from zero to 11 million years, the expected main-sequence lifetime of a B1 star, if they reach the main sequence 36 million years after leaving the spiral arms. These points are then broken into two age categories: zero to 9 million years, the expected main-sequence lifetime of a B0 star, and 10–11 million years, during which only the B1 stars are alive on the main sequence. The points are weighted according to the number of stars seen in each age group. All of the B0 and B1 stars are within 2 kpc of the Sun, as can be seen in Figure 3, and all were launched off the two-armed spiral shock wave with postshock initial velocities. The parameters for the velocity ellipse are

TABLE 2
THE VELOCITY ELLIPSE FOR VARIOUS GROUPS OF STARS IN THE
FILIN (1957) SAMPLE

PARAMETER	GROUP			
	B0-B5	B0-B1	B2-B3	B4-B5
Vertex	$310^\circ \pm 17^\circ$	324 ± 10	306 ± 46	308 ± 22
σ_{π} (km s ⁻¹)	9.9 ± 0.5	10.6 ± 1.2	10.2 ± 0.35	9.7 ± 0.7
σ_{θ_1} (km s ⁻¹)	8.9 ± 0.5	7.5 ± 1.2	9.5 ± 0.35	8.5 ± 0.7

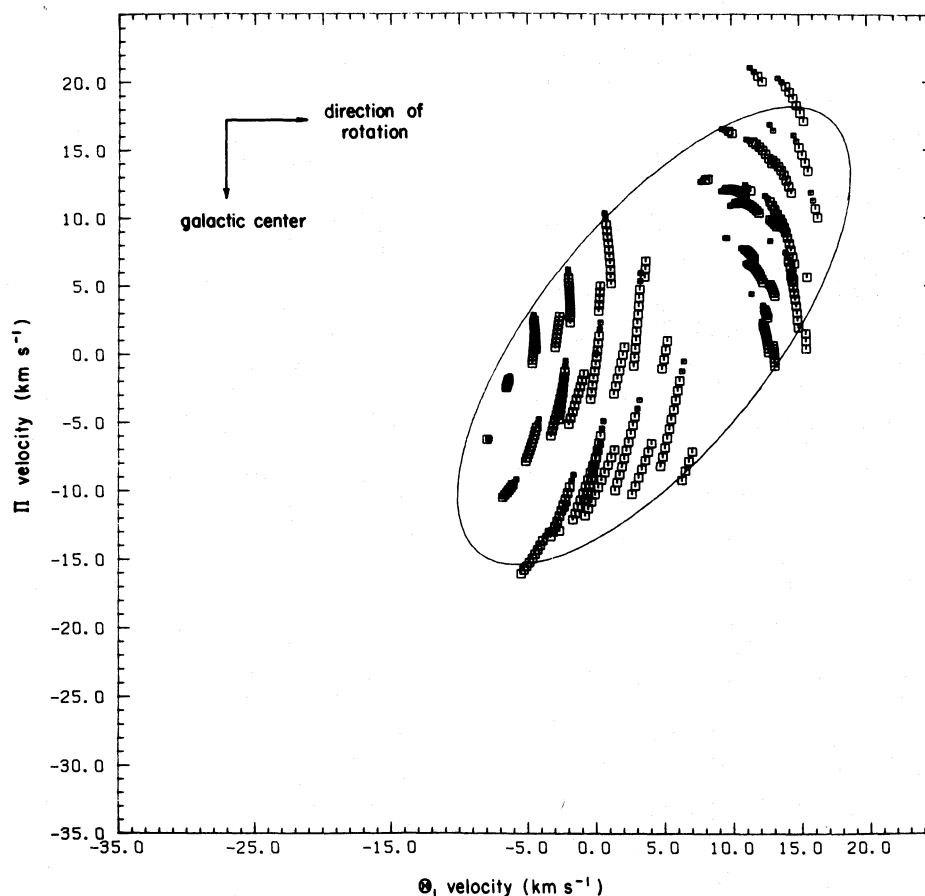


FIG. 2.—The model's velocity distribution of stars launched with post-shock initial velocities having stellar ages from zero to 11×10^6 yr, and assuming that they reach the main sequence 36×10^6 yr after being launched. The size of the plotted symbol is proportional to its weight. The best fitting ellipse is shown where the major and minor axes are 2σ long.

given in Table 3. This sample conforms to the observed B0 + B1 star sample used by Filin (1957). The free parameter, the cloud's age at which stars form, was varied until the model agreed best with the Filin observations of B0 and B1 stars. At a turn-on age of 36 million years, the model vertex is 321° , while Filin observed 324° .

In Figure 2, the ballistic particles are seen along curved tracks, some of which are outside the ellipse. Each track corresponds to ballistic particles launched from a given birth site with a given initial velocity. The birth sites are evenly spaced along the spiral arms. The

squares plotted along each track correspond to different particle ages along the track. The size of the squares shows the weighting. The center of the ellipse is determined by a weighted solution, so the center does not necessarily lie at the center of the patch of points in the figure. Since the major and minor axes of the ellipse drawn in the figures are 2σ long, and since the distribution of particles is not Gaussian, all the points shown do not necessarily lie within the ellipse.

Figure 4 shows essentially the same thing as Figure 2 except that the particles were launched off the two-armed

TABLE 3
THE VELOCITY ELLIPSE FOR VARIOUS GROUPS OF PARTICLES FROM THE GALACTIC MODEL

PARAMETER	AGE GROUP (10^6 yr)			
	Young (0-11)		Middle-aged (0-64)	Older (0-64) (unweighted)
Initial velocities	pre shock	post shock	post shock	post shock
Vertex direction ($^\circ$).....	58	321	324	331
σ_π (km s^{-1}).....	6.6	10.0	9.2	11.6
σ_{θ_1} (km s^{-1}).....	8.2	7.2	7.5	7.7
$\bar{\pi}$ (km s^{-1}).....	-8.6	-8.0	-10.3	-6.3
$\bar{\theta}_1$ (km s^{-1}).....	7.7	16.3	14.0	12.4

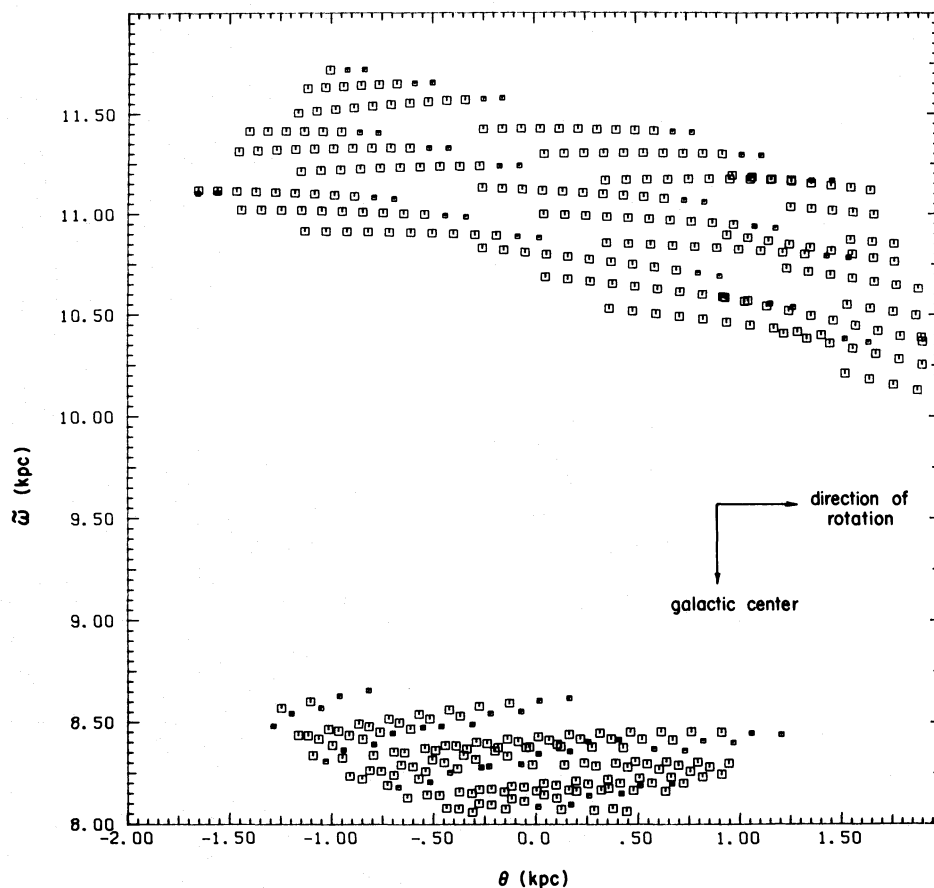


FIG. 3.—The spatial distribution of the stars shown in Fig. 2

spiral shock wave with preshock initial velocities rather than postshock initial velocities. Note that the major axis of the velocity ellipse points at $l = 58^\circ$; thus, preshock initial velocities give a velocity ellipse whose vertex deviation has the wrong sense.

Figure 5 gives the position, in velocity space, of particles with ages from 36 to 100 million years, approximately the expected lifetime of a B5 star on the main sequence. These particles are divided into five age groups corresponding to the expected main-sequence lifetimes of spectral type B0, B1 + B2, B3, B4, and B5 stars and weighted as above. Note that, because of the greater number of particles, especially young, highly weighted particles (see Fig. 1) from the outer spiral arm (the particles on the smaller velocity tracks), the total weighting of these particles is 7.7 times the weighting of the particles from the inner arm. This centers the ellipse on the particles from the outer arm. All these particles are launched off the two-armed spiral shock wave with postshock initial velocities. The velocity ellipse parameters are given in Table 3.

Figure 6 shows the spatial distribution of particles aged 36–100 million years and within 2 kpc of the Sun, the ones whose velocities are shown in Figure 5.

Figure 7 shows the unweighted velocity distribution

and ellipse for particles corresponding to stellar ages from zero to 64 million years launched off the two-armed spiral shock wave with postshock initial velocities. This unweighted ellipse is included because the assumption in the weighting scheme that stars of each spectral type are born simultaneously leads to the younger age groups being more heavily weighted. While the stars with short lifetimes are alive, so are all those with longer lifetimes. The unweighted ellipse gives a better idea of how the weighting scheme affects the velocity ellipse. In the unweighted case, there are equal numbers of particles in each age range. Compared to the weighted cases and to observations of the spectral type distributions of nearby stars, the unweighted cases emphasize stars of later spectral types.

IV. DISCUSSION

In the following discussion, the ellipses will be referred to as young, the B0 and B1 stars (Figs. 2 and 4), middle-aged, the B0 through B5 stars (Fig. 5), and older, the unweighted case which emphasizes the older stars (Fig. 7). Also, postshock initial velocities and preshock initial velocities will be referred to as postshock and preshock respectively.

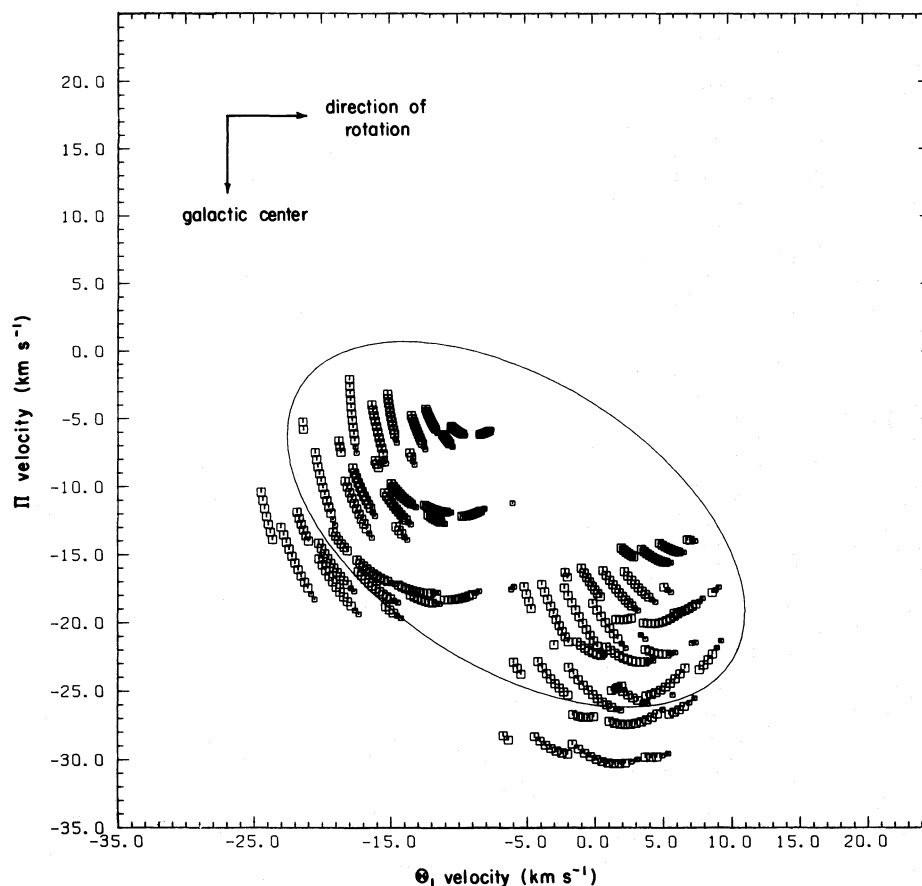


FIG. 4.—Same as Fig. 2, except for preshock initial velocities

a) *The Deviation and Velocity Dispersion of the Ellipses*

The young postshock stars with a modeled vertex deviation of 321° , a π dispersion of 10.0 km s^{-1} , and a θ_1 dispersion of 7.2 km s^{-1} show very good agreement with the values of the vertex deviation and velocity dispersions observed by Filin (1957) for a sample of B0 and B1 stars that had a vertex deviation of 324° , a π dispersion of 10.6 km s^{-1} , and a θ_1 dispersion of 7.5 km s^{-1} . If preshock initial velocities are used, the vertex deviation has the wrong sign. It was not possible to produce a vertex deviation of the correct sign with preshock initial velocities for the young stars while varying the three parameters: position of the Sun with respect to the nearby spiral arms by 10%; the time of formation of the stars by 20 million years; or the lifetime of B0 and B1 stars by 20%. All three age groups of model particles launched with postshock initial velocities show vertex deviations of the same sign as observed and with about the observed size.

The vertex deviation for the postshock particle model, for the young stars mentioned above, was obtained by varying the three parameters: solar position in the Galaxy, the time of formation of stars, and the main-sequence lifetime of B0 and B1 stars to find the best

agreement with the observed velocity ellipse. The best agreement came with the Sun 1.9 kpc away from the inner arm or 1.7 kpc away from the outer arm of the Galaxy (essentially identical to the model of the Galaxy which is assumed in § III), with star formation occurring 36 million years after the clouds are launched off the two-armed spiral shock wave. The distance between the Sun and the local arms of the Galaxy is in good agreement with the solar position calculated from observations by Sharpless (1965). Varying the main-sequence lifetime for B0 and B1 stars by 20% had little effect on the velocity ellipse. Note that, although the Sun is about halfway between two spiral arms in our model, young stars are considerably closer to the Sun on the Perseus arm (anticenter side) than in the direction of the center, and, in a circle of a 2 kpc radius centered on the Sun, there are many fewer stars from the Sagittarius than from the Perseus arm. These effects can be seen clearly in Figure 3. This is due to the assumption, in the ballistic particle model, of a delay between the launching of the parent cloud from the spiral arm and star formation in the cloud, and the initial velocity (postshock) having a radial component directed toward the galactic center. Therefore, young stars are seen a considerable distance inward from the spiral arm which launched them. The time of formation, which represents the age when most but not necessarily

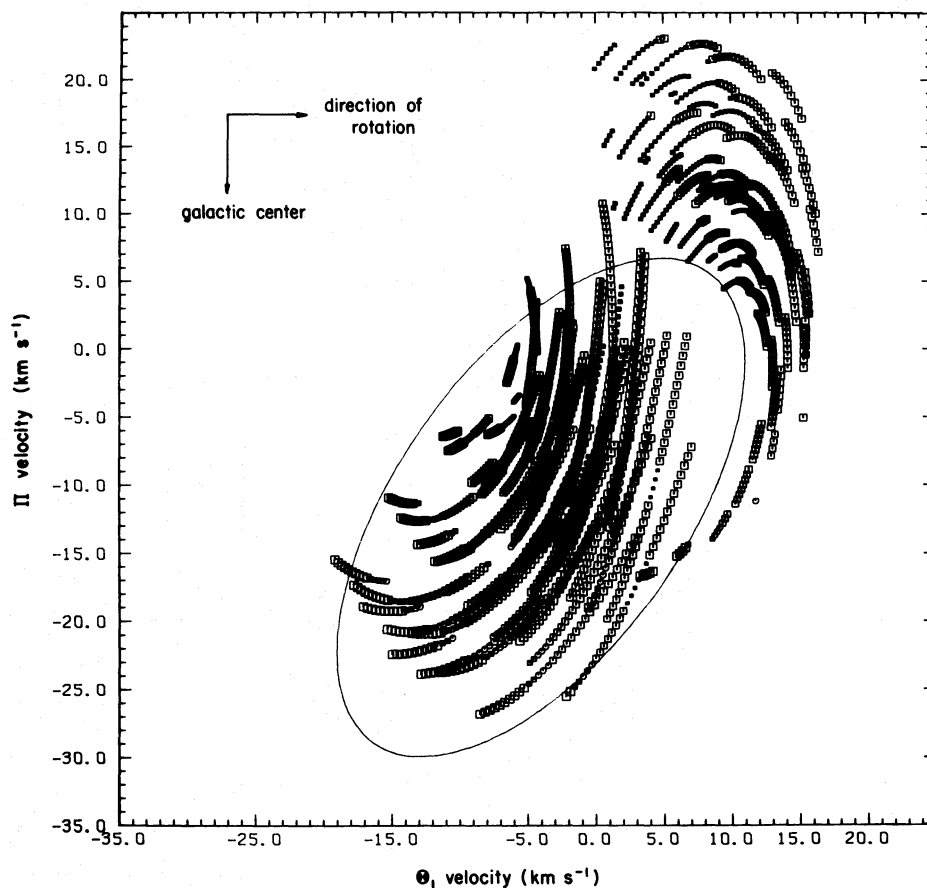


FIG. 5.—Same as Fig. 2, but with stellar ages from zero to 64×10^6 yr

all of the stars are formed, plus the main-sequence lifetime also correlate well with the age of 40 million years calculated by Bash (1979) for the age of stellar clouds when H II regions disappear from them.

Table 3 also includes the value of the solar motion predicted by the model, where we have added the motion of the Sun with respect to the dynamical local standard of rest obtained from Delhaye (1965) to our value of the centroid of the velocity ellipse in the (π, θ_1) plane. The predicted solar motion for the B0–B1 age particles launched with postshock initial velocities agrees well with the velocities calculated from observations of B0 V stars by Delhaye (1965) of $\bar{\pi} = -9.6 \text{ km s}^{-1}$ and $\bar{\theta}_1 = 14.7 \text{ km s}^{-1}$, and the solar motion for the stars in the larger, middle-aged sample launched with postshock initial velocities also agrees with the values of Filin (1957) of $\bar{\pi} = -9.0 \text{ km s}^{-1}$ and $\bar{\theta}_1 = 13.4 \text{ km s}^{-1}$, even though Filin's sample includes a large number of stars from the Orion spur for spectral types B2 through B5.

b) The Change of the Deviation with Age

Finally, it is important to note the change of the deviation of the major axis of the velocity ellipse with time. The vertex of the velocity ellipse for the particles launched with postshock velocities changes very little (7°)

between the young and the old cases. The change of vertex deviation with age and the apparent stability or lack of it can best be understood by thinking of the stars as occurring in two "streams" as was first done by Kapteyn (1900). In this case, the two streams come from the movement of particles from the two arms.

The stream from the outer arm, for particles launched with postshock velocities, is first seen with less than the velocity of the centroid in the $\tilde{\omega}$ and θ directions (point I in Fig. 8). As time passes, the π velocities become smaller by 3 km s^{-1} , while the θ_1 velocities increase by 8 km s^{-1} after about 4 million years (point II). Then, the θ_1 velocities increase by 8 km s^{-1} , while the π velocities increase 20 km s^{-1} at a stellar age of 64 million years (point III). The particles in the inner arm start with greater than average velocities in both the $\tilde{\omega}$ and θ directions (point IV). Then, while the π velocities increase 20 km s^{-1} , the θ_1 velocities decrease 5 km s^{-1} at a stellar age of 55 million years (point V). Finally, θ_1 decreases 10 km s^{-1} , while the π velocities decrease 7 km s^{-1} (point VI). Note that, for the postshock initial velocity model, the initial position of the vertex of the velocity ellipse should change rapidly with time initially, and then, because the change of velocity with time for the older particles occurs along the major axis of the ellipse, there

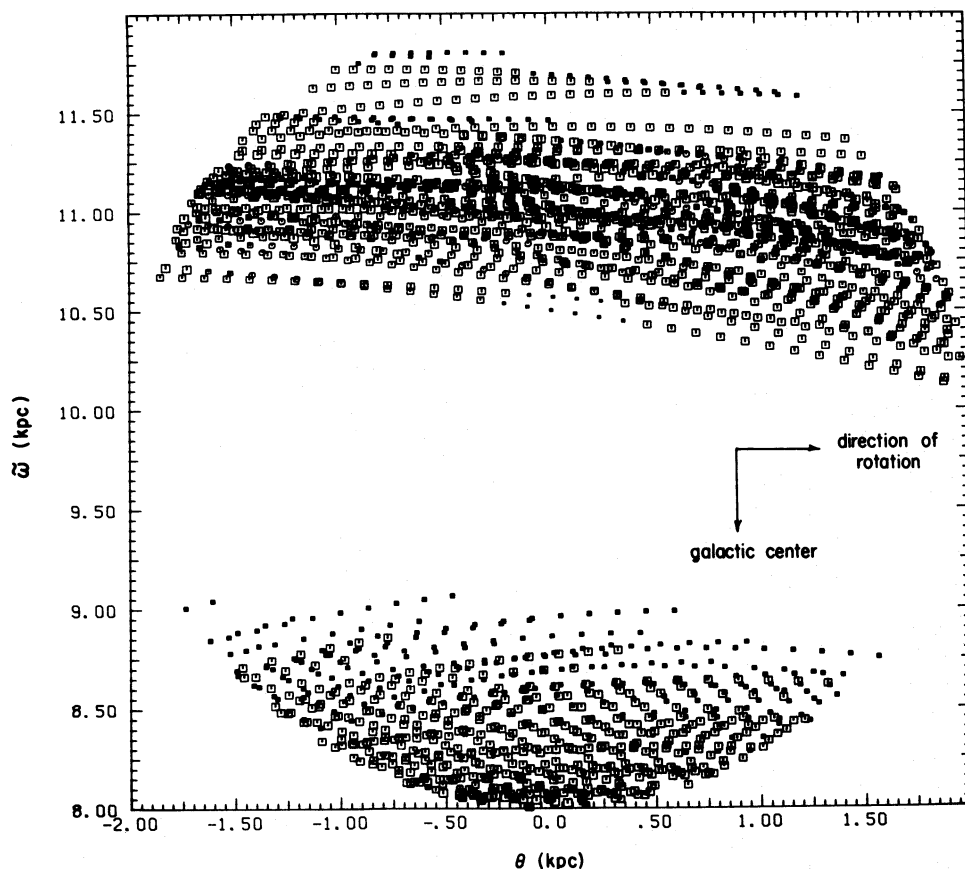


FIG. 6.—The spatial distribution of the stars shown in Fig. 5

should be little change of the position of the vertex of the velocity ellipse. This behavior is seen if one changes the assumed time of formation of early B stars from its best fit time of 36 million years. The vertex of the velocity ellipse stays within 10° of the observed ellipse for at least 11 million years later than the optimum time of formation but is stable for only 3 million years before the best fit formation time. It is also noteworthy that, like the observed velocity ellipse, the dispersions of the π and θ_1 velocities are fairly constant with respect to average age.

The results presented here were produced with a full numerical integration of particle orbits including perturbations by the density wave arms. A qualitative, physical feel for the results can be obtained by ignoring the perturbations and viewing a ballistic particle as moving on a Keplerian ellipse around a central object whose mass is the mass of the Galaxy interior to the launching place. Such a picture is very crude since actual particle orbits are neither closed nor Keplerian ellipses, but instead, in our case, the oldest particle has completed only about one-third of its first orbit. Therefore, the Keplerian ellipse is adequate for giving a qualitative, physical feeling.

The postshock initial velocities have a tangential component slower than the circular velocity and a radial component directed toward the galactic center. Particles launched with this velocity begin their galactic orbits just

past apogalacticon, with those launched farther from the center being launched nearer their apogalactica. The spiral arms which concern us here are the Perseus arm outside the Sun and the Sagittarius arm inside the Sun. We plot the particle velocities in a coordinate system rotating at the circular velocity at the Sun, θ_c . In this coordinate system, the radial velocity out of the Galaxy is the positive π velocity, while the tangential velocity minus the rotational velocity at the Sun is the θ_1 velocity.

Known from the model are the rotation curve of the Galaxy from which we get the mass of the Galaxy, M , seen by the particle at its launching position, the initial π and θ velocities, and the initial distance from the galactic center, r_0 . From these, one can find the orbital semimajor axis length, a , the eccentricity of the orbit, e , the period of the orbit, p , and the initial angle, u_0 , between perigalacticon and the particle as seen from the center of the ellipse.

As the particle moves around the Galaxy, both the π and θ velocities vary according to the following equations:

$$\pi = e \left(\frac{GM}{a} \right)^{1/2} \frac{\sin u}{1 - e \cos u}$$

and

$$\theta = \left(\frac{GM}{a} \right)^{1/2} \frac{(1 - e^2)^{1/2}}{1 - e \cos u},$$

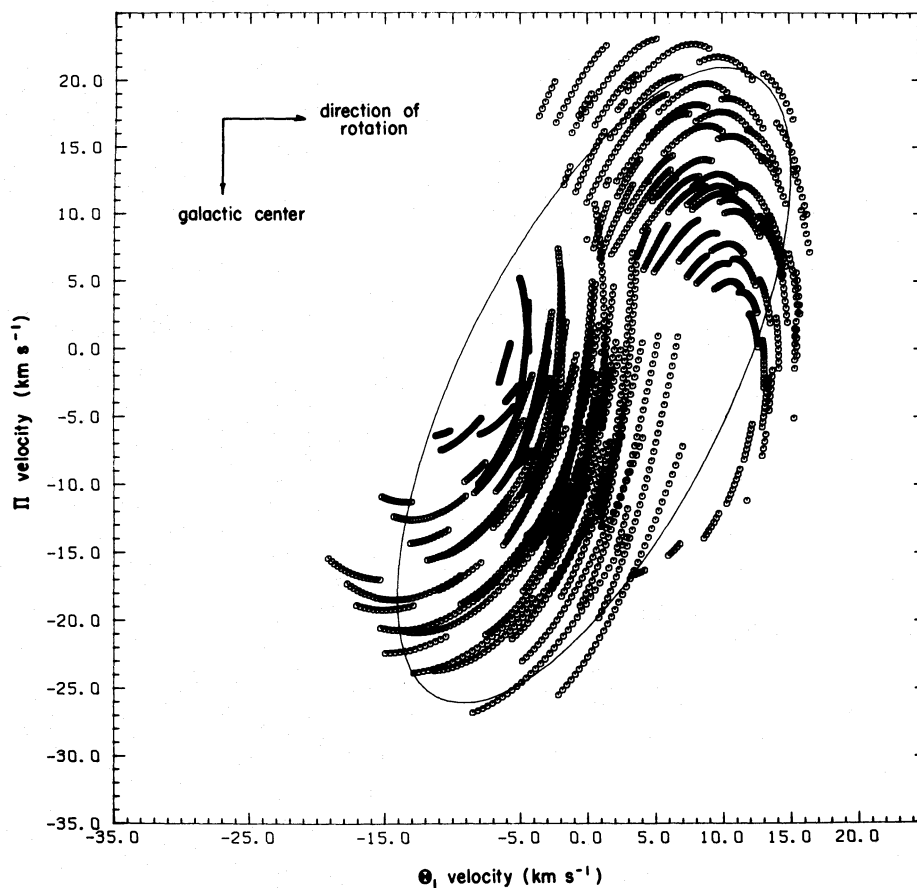


FIG. 7.—The equal-weighted velocity distribution of stars launched with postshock initial velocities and stellar ages from zero to 64×10^6 yr. Same as Fig. 5, but with all model stars weighted equally.

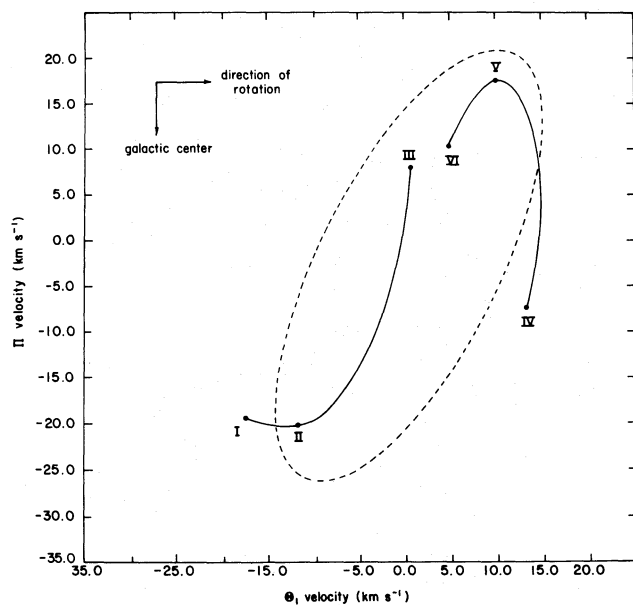


FIG. 8.—A schematic representation of the change of velocity with age for stars launched with postshock initial velocities. The stars from the Perseus arm move along the track labeled I, II, III. Those from the Sagittarius arm move along the track labeled IV, V, VI.

where $(GM/a)^{1/2}$ is the circular velocity at distance a . In our case, all the Keplerian orbits have $e \lesssim 0.1$, and, for such small values of e , this Keplerian picture is a good approximation.

The Keplerian picture predicts that ballistic particles from the outer and inner arms will each move in velocity in a (π, θ_1) diagram along ellipse-like tracks. The center of each ellipse-like figure lies at $\pi \approx 0$ and at a θ_1 velocity equal to the difference between the circular velocity at the Sun and the circular velocity at the particle's mean distance from the center. These ellipse-like figures can be seen in Figure 8, but since the particle takes one orbital period to complete its ellipse-like velocity figure, our particles are seen to complete only a fraction of their figures. In the numerical models (Figs. 2, 4, 5, 7, and 8), the centers of the ellipse-like figures are found to lie at $\theta_1 = +8 \text{ km s}^{-1}$ for the inner arm and $\theta_1 = -12 \text{ km s}^{-1}$ for the outer arm. Our Keplerian picture predicts 10 km s^{-1} for the inner arm and -11 km s^{-1} for the outer arm.

Finally, although particles from both the arms are launched at about the same initial angle, U_0 , in their orbit, the tracks for the stars start at very different points. This difference is caused by the difference in orbital period for particles in the two arms; 171×10^6 years for the inner arm and 274×10^6 years for the outer arm in the

Keplerian approximation. Since the formation time for stars is the same in both arms, those particles representing stars from the outer arm start at a point farther around the track than where the particles from the inner arm start. The point where the tracks begin in Figure 8 agrees with expected velocities in the Keplerian approximation of the model. Thus, the velocity tracks in Figure 8 are seen to have starting velocities that are quite predictable from the Keplerian picture, and the specific length of each velocity track is also predicted by the Keplerian model. The amplitudes for these functions are 35 km s^{-1} for the θ_1 velocity and 38 km s^{-1} for the π velocity for the inner arm of the Galaxy, and 18 km s^{-1} for the θ_1 velocity and 20 km s^{-1} for the π velocity for the outer arm of the Galaxy. We can see that the change in velocity given by the Keplerian approximation is about a factor of 2 too high for the inner arm but is just about right for the outer arm.

V. SUMMARY

We assumed the ballistic particle model which asserts that spiral arm stars form in dense clouds launched from the arms and that the orbits of both clouds and stars are known. That model, for the Galaxy, also includes the location of the Sun relative to the nearby main spiral arms. We assumed three free parameters: (1) the time, after the clouds leave the spiral arms, at which the stars, forming in the cloud, reach the main sequence; (2) the position of the Sun relative to the arms; and (3) the main-sequence lifetimes of B0 through B5 stars. We varied the three free parameters until we obtained the best agreement between the model and observations of B0 and B1 stars. The best agreement was achieved when we assumed a delay of 36 million years from the birth of the clouds in the arms to the birth of the stars in the cloud. Agreement with observations is sensitively dependent on the assumed location of the Sun with respect to the spiral

arms, and best agreement was achieved at the Sun's location in the ballistic particle model for the Galaxy (Bash and Peters 1976). The results are not sensitive to variation of assumed main-sequence lifetimes for B0 through B5 stars by 20%.

The ballistic particle model predicts a velocity distribution for young stars in the solar vicinity which agrees quite well with observations. In that model, stars form in molecular clouds which have been launched from spiral arms at postshock velocities. If we use preshock initial velocities, a velocity ellipse vertex deviation of the wrong sign is seen.

Thus, the ballistic particle model offers an explanation for the presence of the vertex deviation and the sense and amount of the deviation. The model velocity ellipse which fits the observations best also agrees very well with the ages of the particles that have been suggested in previous papers (e.g., Bash 1979) to correspond with H II regions.

It was not possible to confirm the deviation of the velocity ellipse for stars of spectral types later than B1 because of contamination due to the stars that have formed from the Orion spur in the Galaxy; this spur is not in our model. However, the velocity ellipses formed from particles with postshock initial velocities do show some of the properties of the observed velocity ellipse for later spectral type stars, as late as B5: (1) the deviation of the major axis of the velocity ellipse does not change significantly with the addition of older stars; (2) the deviation is definitely negative for all ages; (3) the dispersions, σ_π and σ_{θ_1} , are fairly constant with stellar age; and (4) the mean π and θ_1 velocities agree with the observed mean velocities. The particles launched with preshock initial velocities showed none of these properties. It may be possible, in the next stage of our investigation of the velocity ellipse, to model the effects of the local spur of the Galaxy and see how the stars formed from it affect the velocity ellipse.

REFERENCES

- Bash, F. N. 1979, *Ap. J.*, **233**, 524.
 Bash, F. N., Green, E., and Peters, W. L. 1977, *Ap. J.*, **217**, 464.
 Bash, F. N., and Peters, W. L. 1976, *Ap. J.*, **205**, 786.
 Cester, B. 1965, *Zs. Ap.*, **62**, 191.
 Delhaye, J. 1965, in *Stars and Stellar Systems*, Vol. 5, *Galactic Structure*, ed. W. A. Blauu and M. Schmidt (Chicago: University of Chicago Press), p. 61.
 Filin, A. Ia. 1957, *Astr. Zh.*, **34**, 525 (English transl. in *Soviet Astr.—AJ*, **1**, 517).
 Heckmann, O., and Strassl, H. 1934, *Veroff. U. Sternw. Göttingen*, No. 41.
 House, F. C., and Innanen, K. A. 1975, *Ap. Space Sci.*, **32**, 139.
 Kapteyn, J. C. 1900, *Congress of Arts and Sciences*, St. Louis, **4**, 413.
 ———. 1922, *Ap. J.*, **55**, 302.
 Lesh, J. R. 1968, *Ap. J. Suppl.*, **17**, 371.
 ———. 1972, *Astr. Ap. Suppl.*, **5**, 129.
 Lindblad, B. 1927, *Medd. Uppsala Astr. Obs.*, No. 14.
 Mayor, M. 1970, *Astr. Ap.*, **6**, 60.
 Nordström, H. 1936, *Medd. Lunds Astr. Obs.*, No. 79.
 Oort, J. H. 1928, *Bull. Astr. Inst. Netherlands*, **4**, 269.
 Schwarzschild, K. 1908, *Nachr. Königl. ges. wiss. Göttingen*, No. 2, p. 191.
 Sharpless, S. 1965, in *Stars and Stellar Systems*, Vol. 5, *Galactic Structure*, ed. W. A. Blauu and M. Schmidt (Chicago: University of Chicago Press), 131.
 Shu, F. H., Milione, V., and Roberts, W. W., Jr. 1973, *Ap. J.*, **183**, 819.
 Strothers, R. 1974, *Ap. J.*, **194**, 651.
 Wielen, R. 1977, in *IAU Symposium 77, Structure and Properties of Nearby Clusters*, ed. E. M. Berkhuijsen and R. Wielebinski (Dordrecht: Reidel), p. 93.
 Woolley, R. 1970, in *IAU Symposium 38, The Spiral Structure of Our Galaxy*, ed. W. Becker and G. Contopoulos (Dordrecht: Reidel), p. 423.
 Yuan, C. 1969, *Ap. J.*, **158**, 889.
 ———. 1971, *Ap. J.*, **176**, 664.

FRANK BASH and JAMES L. HILTON: Astronomy Department, University of Texas at Austin, R. L. Moore Building, Austin, TX 78712